

PAPER • OPEN ACCESS

## Study on the Adsorption Performance of Biochar/Montmorillonite Composites for Ciprofloxacin Hydrochloride

To cite this article: Xinpeng Wei *et al* 2024 *J. Phys.: Conf. Ser.* **2920** 012010

View the [article online](#) for updates and enhancements.

You may also like

- [Molecular Dynamics Study of the Bonding Mechanism at the Epoxy/Concrete Interface](#)  
Jianzhong Wang, Jeremiah Millare, Zhenjun Nie *et al.*
- [Atmospheric Pressure Nitrogen Corona Discharge and Its Application in Hydrophilicity Modification of Polypropylene Fibber Surfaces](#)  
Guangda Yang, Fuzi Zhang, Hongfei Zhang *et al.*
- [Microscopic Simulation Study on Orientation Degree of PBO Fiber Macromolecular Chains](#)  
Haiyun Zhang, Danyong Wang, Shuhu Li *et al.*



**UNITED THROUGH SCIENCE & TECHNOLOGY**

 **The Electrochemical Society**  
Advancing solid state & electrochemical science & technology

**248th  
ECS Meeting**  
Chicago, IL  
October 12-16, 2025  
*Hilton Chicago*

**Science +  
Technology +  
YOU!**

**SUBMIT  
ABSTRACTS by  
March 28, 2025**

**SUBMIT NOW**

The advertisement features a central image of a smiling woman with long dark hair, wearing a brown blazer, gesturing with her hands. The background is a blue gradient with a network of white dots and lines. The banner is framed by a decorative border of circular icons at the top and bottom.

# Study on the Adsorption Performance of Biochar/Montmorillonite Composites for Ciprofloxacin Hydrochloride

Xinpeng Wei <sup>\*1</sup>, Yanxia Zhang <sup>2</sup>, Zhiyong Han <sup>\*1</sup>, Zixuan Wang <sup>1</sup>, Kexin Wang <sup>1</sup>, Ao Xian <sup>1</sup>

1 School of Petrochemical Engineering, Lanzhou University of Technology, Gansu 730050, China;

2 Datang Shaanxi power generation Co., Ltd. Weihe thermal power plant, Shaanxi 712085, China

\*Corresponding author's e-mail: hanzhy\_009@sina.com

\*First author's e-mail: wxp1020865042@126.com

**Abstract:** In response to the widespread and difficult-to-treat phenomenon of antibiotic pollution by ciprofloxacin hydrochloride, this study has chosen to adopt a simple and efficient adsorption method for its treatment and innovatively proposed a method for preparing biochar/montmorillonite composites through pyrolysis and intercalation methods for adsorption treatment. The study also analyzes factors affecting the adsorption effect as well as the adsorption thermodynamics and kinetics characteristics, aiming to provide new efficient and low-cost technologies and ideas for the treatment of antibiotic wastewater. And the research indicates:

a) Compared to single biochar and montmorillonite, the specific surface area of biochar/montmorillonite composites has significantly increased, with C2M1C reaching 246.729 m<sup>2</sup>.g<sup>-1</sup>, which is 91% higher than ZBC. The reason is that the composite material's surface has both the layered structure of montmorillonite and the tubular pore structure of biochar.

b) The optimal ratios for preparing composites by pyrolysis and intercalation methods are 1.5:1 and 2:1, respectively, and composites prepared at these ratios exhibit the best adsorption effect for CIP.

c) Composite materials are more suitable for CIP adsorption in alkaline environments (with an optimal pH value of 10).

d) The adsorption capacity of CIP increases with time, initial concentration, and temperature.

e) The adsorption capacity of composite materials for CIP decreases significantly with an increase in the number of cycles. The adsorption amounts of materials R1.5M1D and intercalated composite material C2M1C dropped from 89.457 and 114.782 mg g<sup>-1</sup> during the first cycle to 16.237 and 24.353 mg g<sup>-1</sup> in the fifth cycle, with decreases of 81% and 78%, respectively.

## 1. Introduction

Antibiotic wastewater mainly comes from the antibiotic production process, including microbial fermentation, filtration, extraction, crystallization, refining, and refinement processes. This type of wastewater is characterized by high COD content, complex composition, and the presence of residual antibiotics. Antibiotic pollution is one of the four emerging pollutants, and residues of ciprofloxacin



hydrochloride, a commonly used broad-spectrum antibiotic, in the environment may lead to the spread of antibiotic resistance. Therefore, the removal of ciprofloxacin hydrochloride from water bodies is critical for environmental protection and public health. The removal of ciprofloxacin hydrochloride can be done in the following ways:

- a) **Advanced Oxidation Process:** Advanced Oxidation Processes (AOPs) mineralize organic pollutants by generating strong oxidants such as hydroxyl radicals. Examples include Fenton, multiphase photocatalysis, and ozone oxidation, which may require high energy input and specific reaction conditions [1].
- b) **Iron oxide activated persulfate:** Iron oxides can activate persulfate to produce sulfate and hydroxyl radicals, and these reactive oxygen species can efficiently degrade ciprofloxacin hydrochloride. In which recovery and recycling of the catalyst may be one of the challenges [2].
- c) **Magnetized nitrogen-doped biochar-activated peroxydisulfate:** Magnetized nitrogen-doped biochar (MNBC) was used as an activator for peroxydisulfate (PMS) with good stability and magnetic properties for easy separation and recovery. However, the preparation cost and performance of the catalyst may need to be further optimized [3].
- d) **Photocatalysts** can catalyze the degradation of ciprofloxacin hydrochloride under visible light irradiation, but the recycling performance may be poor, which limits their economy in practical applications [4].
- e) **Adsorption:** Biochar is a porous carbon material prepared by pyrolysis of organic materials with high specific surface area and rich surface functional groups, which can effectively adsorb ciprofloxacin hydrochloride. For example, the adsorption and removal rate of ciprofloxacin hydrochloride by biochar prepared by pyrolysis of kitchen anaerobic digestate biochar at 700 °C (DR-700) can reach 95.09%. [5].

The advantages of biochar adsorption are the relatively low cost and the possibility of utilizing resources such as agricultural wastes, but the adsorption efficiency may be affected by factors such as solution pH, temperature, and the specific surface area of the biochar. Considering the advantages, disadvantages, and cost analysis of the above methods, this study adopted the idea of preparing composite adsorbent materials with biochar and montmorillonite for the adsorption and removal of antibiotics, with a view to providing new ideas for the effective treatment of antibiotic pollutants.

## 2. Materials and Methods

### 2.1 Experimental Material

#### 2.1.1 Raw materials for the preparation of biochar/montmorillonite composites

Biochar prepared from montmorillonite and rice husk was used as the raw material for the composites in this experiment, where rice husk was purchased from farmers' markets and montmorillonite was purchased directly from the chemical company.

#### 2.1.2 Laboratory reagents and instruments

The reagents and apparatus used in the experiment are shown in Tables 1 and 2 below.

drug name	molecular formula	fineness	manufacturer (of a product)
<b>Nitrogen</b>	N <sub>2</sub>	99.90~99.95%	Lanzhou Yulong Gas Co.
<b>Potassium dichromate</b>	K <sub>2</sub> Cr <sub>2</sub> O <sub>7</sub>	Analytically pure	Shanghai McLean Biotechnology Co.
<b>Ciprofloxacin hydrochloride</b>	C <sub>17</sub> H <sub>18</sub> FN <sub>3</sub> O <sub>3</sub> ·HCl	Analytically pure	Shanghai Aladdin Biochemical Technology Co.
<b>Sodium hydroxide</b>	NaOH	Analytically pure	Guangdong Guanghua Technology Co.
<b>Hydrochloric acid</b>	HCl	Analytically pure	Shanghai Aladdin Biochemical Technology Co.
<b>Nitric acid</b>	HNO <sub>3</sub>	Analytically pure	Shanghai Aladdin Biochemical Technology Co.
<b>Phosphoric acid</b>	H <sub>3</sub> PO <sub>4</sub>	Analytically pure	Tianjin Fuyu Fine Chemical Co.

<b>Sulfuric acid</b>	H <sub>2</sub> SO <sub>4</sub>	Analytically pure	Black Medicine Group Chemical Reagent Co.
<b>Zinc chloride</b>	ZnCl <sub>2</sub>	Analytically pure	Shanghai McLean Biotechnology Co.
<b>Ultra-pure water</b>	H <sub>2</sub> O	Analytically pure	Laboratory self-made
<b>Dibenzoyl dihydrazide</b>	C <sub>13</sub> H <sub>14</sub> N <sub>4</sub> O	Analytically pure	Tianjin Tianxin Fine Chemical
<b>Methanol</b>	CH <sub>3</sub> OH	Analytically pure	Lee On Lung Pok Wah Pharmaceutical & Chemical Co.
<b>Montmorillonite</b>	Al <sub>2</sub> SiO <sub>10</sub> (OH)·H <sub>2</sub> O	Analytically pure	Shanlin Shi Shi Mineral Products Co.

Table 1 Experimental reagentst

Instrument Name	model number	manufacturer (of a product)
tube furnace	OTF-1200X	Hefei Kejing Material Technology Co.
High-speed universal pulverizer	FW100	Tianjin Tester Instrument Co.
ultraviolet-visible spectrophotometer	752	Shanghai Sunyu Hengping Scientific Instrument Co.
temperature controlled shaker	SKY-200B	Shanghai Sukun Industrial Co.
Electrothermal blast drying oven	HGZF-101-1	Shanghai Yuejin Medical Equipment Co.
Circulating water type multi-purpose vacuum pump	SHB-3	Zhengzhou Dufu Instrument Factory
electronic balance	FA2004	Shanghai Liangping Instrumentation Co.
magnetic stirrer	HJ-4A	Changzhou Guohua Electric Co.
water bath	HH-2A	Beijing Kewei Yongxing Instrument Co.
Benchtop centrifuge	TA2-16K	Shanghai Dam Industrial Co.
X-ray diffractometer	BrukerAXS D8	Bruker, Germany
BET Surface Analyzer	MicromeriticsASAP2460	Micromeritics
Fourier infrared spectroscopy	Thermo Scientific Nicolet iS5	Thermo Fisher Scientific (China) Co.

Table 2 Experimental equipmen

## 2.2 Experimental Methods

### 2.2.1 Preparation of experimental materials

(1) *Preparation of rice husk charcoal.* After washing the rice husk impurities, it is dried in a blast drying oven. The dried rice husk was processed by a high-speed pulverizer and screened through a 200-mesh screen. The screened rice husk was mixed with a 55% ZnCl<sub>2</sub> solution at a ratio of 1:1, dried, put into a corundum boat, placed in a tube furnace. The biochar was produced by pyrolyzing under nitrogen at 400°C for 4h at a heating rate of 20°C/min. After pyrolysis, it was cooled to room temperature and removed.

(2) *Preparation of composites by pyrolysis.* Montmorillonite was mixed with biochar in mass ratios of 2:1, 1.5:1, 1:1, and 1:1.5 in a corundum boat. The corundum boat was shaken to ensure that the materials were mixed, and then the composites were synthesized by placing them in a tube furnace at 400°C under nitrogen and heating them at a rate of 20°C/min for 4 h. After pyrolysis, the samples were naturally cooled to room temperature.

(3) *Preparation of composites by the intercalation method.* Sodium-based montmorillonite was mixed with distilled water at a ratio of 1:30 (m/V) and stirred for 2 h. Next, rice husk charcoal with mass ratios of montmorillonite: biochar 2:1, 1.5:1, 1:1, and 1:1.5, respectively, was added into a 6% NaOH solution at a ratio of 1:30 and stirred for 30 min to form a suspension. The suspension was poured into the montmorillonite solution and continued stirring for 5 h. Afterwards, it was centrifuged, washed to neutral, dried, and ground through a sieve for subsequent use.

### 2.2.2 Adsorption experiment

This study provides an in-depth investigation of the adsorption performance of biochar/montmorillonite composites by examining single-factor variables such as adsorption thermodynamics, adsorption isotherms, adsorbent pH, and dosage.

(1) *Effect of adsorbent composite ratio on adsorption.* Accurately weighed 0.01 g of the composites prepared by pyrolysis and intercalation, with the same composite ratios of montmorillonite to biochar of 2:1, 1.5:1, 1:1, and 1:1.5. These composites were transferred into containers containing 100 mL of ciprofloxacin hydrochloride solution with a concentration of 30 mg/L, respectively, and were rotated at a temperature set at 25 °C and a rotational speed of 180 r/min. Oscillate in an oscillation chamber for 4 hours and ensure that the mouth of the bottle is closed to prevent changes in the concentration of the solution due to the evaporation of water. The mixture was filtered using a 10 mL syringe with a disposable needle filter, and an appropriate amount of the filtrate was placed in a UV spectrophotometer to determine its absorbance, and the concentration of the solution was calculated accordingly to determine the optimal compounding ratio.

(2) *Effect of adsorbent dosage on adsorption.* In this study, the effect of different quantities of composites on the adsorption properties of ciprofloxacin hydrochloride was investigated under specific experimental conditions. The details of the experiment are as follows: For ciprofloxacin hydrochloride solution, the volume was set to 100 mL and the concentration was 30 mg/L. The experiment was also carried out at 25 °C, the adsorption time was 4 h, the pH was kept in the natural state, and the speed of the shaker was 180 r/min. The experiments were evaluated to assess the effect of the composites dosage at the levels of 0.005, 0.010, 0.015, 0.020, and 0.025 g on the adsorption performance of ciprofloxacin hydrochloride.

(3) *Effect of solution pH on adsorption.* Ciprofloxacin hydrochloride solution in a volume of 100 mL, concentration of 30 mg/L, temperature of 25 °C, adsorption time of 4 h, using 0.025 g pyrolysis composite R1.5M1D and 0.02 g intercalation composite C2M1C, and a shaker speed of 180 rpm, was used to adjust the pH value by a standard solution of 1 mol/L HCl and NaOH to 2, 4, 6, 8, and 10 on the adsorption properties of different composites.

(4) *Effect of initial solution concentration, temperature and reaction time on adsorption.* The initial concentration of the adsorbent solution, the temperature, and the reaction time as experimental conditions have similar effects on the adsorption process as those studied in adsorption kinetics and adsorption isotherms.

(5) *Adsorption isotherms and adsorption thermodynamics.* For the ciprofloxacin hydrochloride solution, the experimental conditions were set at 100 mL with concentrations of 10, 15, 20, 25, and 30 mg/L in that order; the pH was set at 10, and the temperature gradients were 15°C, 25°C, and 35°C. 0.025 g of pyrolysis composite R1.5M1D and 0.02 g of intercalation composite C2M1C were added to a conical flask at 180 rpm and shaken in a shaker for 4 h.

(6) *Reaction time and adsorption kinetics.* In the experiment, the solution volume was set to be 50 mL with a concentration of 50 mg/L and a temperature of 25 °C. 0.015 g of pyrolysis composite R2M1D and 0.01 g of intercalation composite C1M1C were added, respectively, the pH was adjusted to 10, and the speed of the shaking machine was set at 180 r/min. Under these conditions, the sampling times were carried out at 5, 10, 20, 40, 60, 90, 120, 150, 180, 240, and 300 min of continuous sampling. After each sampling, the concentration  $C_t$  of the solution, which is the concentration at a specific time point  $t$ , was determined. Based on the obtained data, the adsorption amount  $q_t$  at time point  $t$  was calculated, which in turn was used to construct an adsorption kinetic model.

(7) *Biochar recycling performance.* By desorbing the adsorbent from the adsorbent, the composites were recycled, thus realizing the goal of reducing the economic cost. The experimental steps were as follows: first, the adsorption-saturated composites were filtered out of the solution, and then placed in 0.01 mol/L HCl solution for desorption for 4 h. Next, the composites were separated and cleaned with ultrapure water, and then put into an oven for drying treatment so that they could be used for adsorption again. After five cycles of adsorption, the absorbance was determined and thus the adsorbed amount was calculated and analyzed for comparison.

### 3. Results and Analysis

#### 3.1 Characterization of Biochar/Montmorillonite Composites

To investigate the microstructural changes of the composites before and after adsorption, the materials were characterized by SEM, XRD, BET, and FTIR.

##### 3.1.1 SEM Analysis

Figures 1-(a) and (b) show the SEM images of the composites R1.5M1D, C2M1C magnified 500, 5000 and 10000 times, respectively.

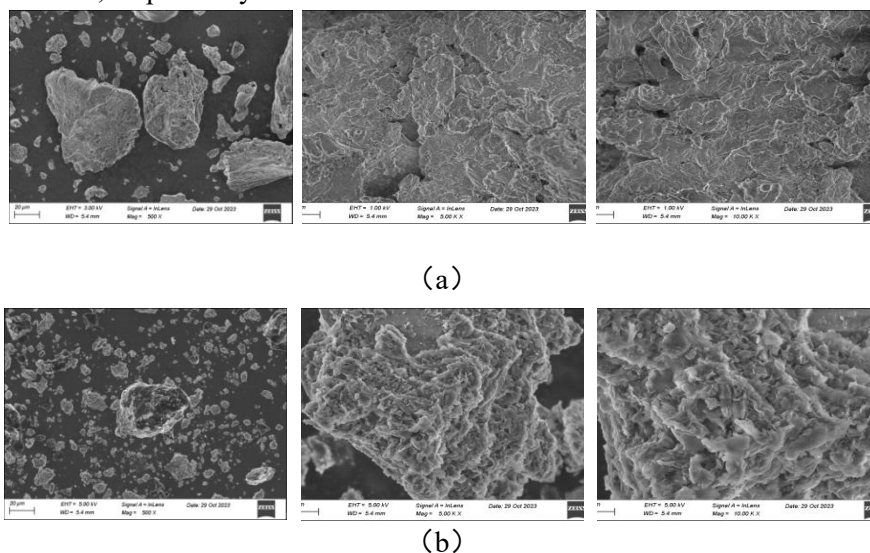


Figure 1 Scanning electron microscopy of R1.5M1D and C2M1C

Figure 1-(a) shows that the pyrolyzed composite R1.5M1D has a rough surface with deep pores visible at 5000x magnification, and many pores and obvious laminar structure at 10000x, which increases its adsorption capacity for ciprofloxacin hydrochloride. And Figure 1-(b) shows that the particle state of C2M1C intercalation composites is similar to the aforementioned materials at 500 times magnification. At 5000 times magnification, its surface was rough and porous, containing a large number of flakes of different shapes and sizes. At 10,000-fold magnification, the complex structure of pores and flakes and the high specific surface area characteristics were more significant, which significantly enhanced the adsorption removal rate of MT and ZBC. Meanwhile, the surface of C2M1C is rougher than that of the pyrolyzed composite R1.5M1D.

##### 3.1.2 XRD Analysis

According to Figure 2, ZBC did not show significant diffraction peaks in the range of 20 to 30 degrees, whereas both MT and composites exhibited significant diffraction peaks, indicating that the biochar and montmorillonite have been successfully composited. The diffraction peak of ZnC was observed at  $2\theta = 34$  degrees, which is consistent with the characterization of ZnCl<sub>2</sub>-modified biochar. At  $2\theta$  between 26 and 28 degrees, the MT showed diffraction peaks consistent with SiC, which matched the typical Si diffraction peaks of montmorillonite. The composite R1.5M1D showed a diffraction peak matching S at  $2\theta$  approximately equal to 28 degrees, while C2M1C showed a typical Zn diffraction peak at  $2\theta$  approximately equal to 30 degrees, which is consistent with the characteristics of ZnCl<sub>2</sub>-modified biochar. After adsorption of CIP, the intercalated and pyrolyzed composites ACCIP and ARCIP showed diffraction peaks matching C<sub>3</sub>N<sub>4</sub> between 26 and 35 degrees, from which it can be inferred that the nitrogen element in them mainly originated from CIP.

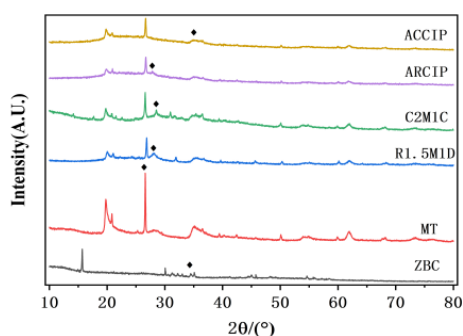


Figure 2 Test spectrum of XRD

### 3.1.3 BET Analysis

The specific surface area of modified biochar ZBC, montmorillonite MT, pyrolysis composite R1.5M1D, and intercalation composite C2M1C were analyzed respectively, and the data are shown in Table 3.

Name of material	specific surface area (m <sup>2</sup> /g)	Total Hole Volume (cm <sup>3</sup> /g)	Average pore size (nm)
ZBC	5.29	0.02	10.48
MT	66.59	0.15	9.99
R1.5M1D	86.28	0.03	23.66
C2M1C	246.73	0.22	5.80

Table 3 Pore structure data of ZBC、MT、R1.5M1D、C2M1C

According to Table 3, the specific surface area of the composites was significantly higher than that of the single materials ZBC and MT. In particular, the pyrolytic composite R1.5M1D and the intercalated composite C2M1C showed an enhancement of 94% and 98% to 86.2830 m<sup>2</sup>.g<sup>-1</sup> and 246.7287 m<sup>2</sup>.g<sup>-1</sup>, respectively, the total pore volume of the intercalated composite C2M1C of 0.218292 cm<sup>3</sup>.g<sup>-1</sup>, which is the largest of all the materials with a 91% improvement. The pyrolytic composite R1.5M1D had the largest average pore size of 23.655 nm. This indicates that the composite of ZBC and MT can effectively improve the insufficient specific surface area and total pore volume of a single material, provide better pore structure for CIP adsorption, increase the surface area and pore volume of the composite, and favor the adsorption of CIP molecules [6].

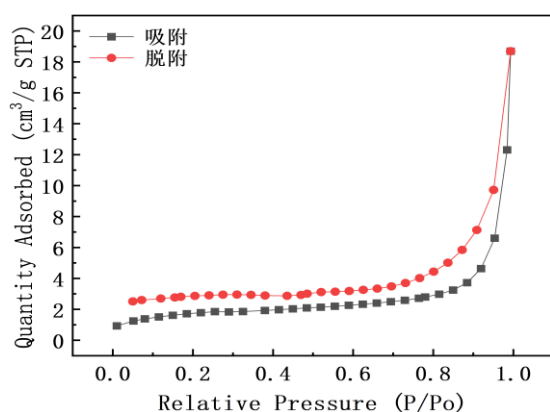


Figure 3 Adsorption and desorption curves of R1.5M1D

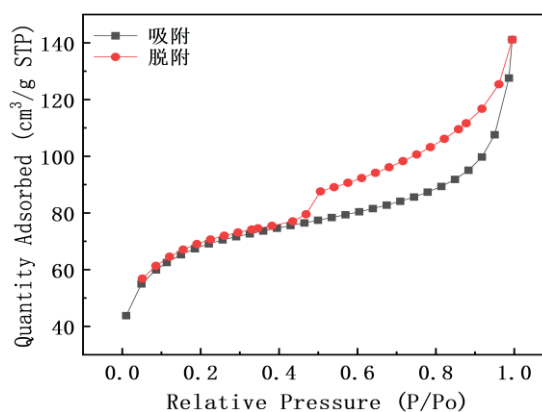


Figure 4 Adsorption and desorption curves of C2M1C

Figures 3 and 4 show the adsorption and desorption curves for R1.5M1D and C2M1C, respectively. The C2M1C curve exhibits an H3-type hysteresis loop, whereas the R1.5M1D curve is not closed, which implies the inhomogeneity of the adsorbent's pore structure and the contraction of the biochar's pore size, and belongs to the isotherms of type II. The ZBC, MT, and C1M1C curves belong to type IV, which suggests the unilamellar and multilamellar adsorption, as well as

the capillary condensation presence of the phenomenon.

### 3.1.4 FTIR Analysis

The Fourier transform infrared spectra of ZBC, MT, R1.5M1D and C2M1C are plotted in Figure 5.

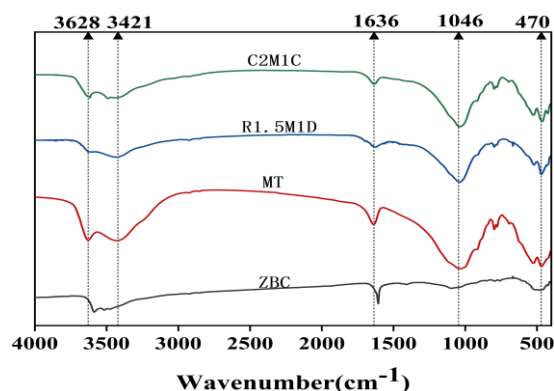


Figure 5 FTIR spectra of ZBC 、 MT 、 R1.5M1D and C2M1C

According to Figure 5, the Fourier transform infrared spectrograms of MT, R1.5M1D, and C2M1C showed high similarity and significant differences with those of ZBC. ZBC did not show vibrational peaks in the wave number range of 1000 to 500  $\text{cm}^{-1}$ , which indicates that the peaks in the composites are due to MT composite and further suggests that MT is tightly bound to the biochar. All four composites showed peaks formed by -OH stretching vibration at 3628  $\text{cm}^{-1}$  and N-H absorption peak at 3421  $\text{cm}^{-1}$ , which indicates that the composited materials contain nitrogen. A single peak formed by C=C, C=O telescopic vibration is present at 1639  $\text{cm}^{-1}$  and a peak formed by Si-O telescopic vibration is present at 1046  $\text{cm}^{-1}$ , which coincides with the characteristic peaks of montmorillonite. The presence of peaks in the wave number range from 1500 to 400  $\text{cm}^{-1}$  indicates the presence of single bond vibrations. The peak at 470  $\text{cm}^{-1}$ , on the other hand, mainly reflects the bending vibrational mode of silicon-oxygen bonds (Si-O).

## 3.2 Adsorption Properties Exploration

### 3.2.1 Effect of composite ratio on adsorption effect

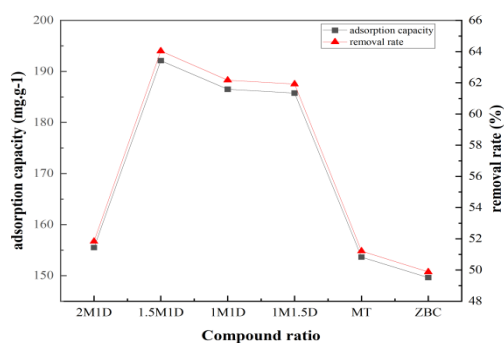


Figure 6 The effect of composite ratio on the adsorption of CIP by the pyrolytic composite R1.5M1D

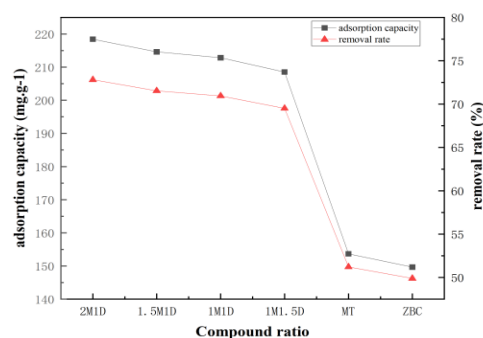


Figure 7 The effect of composite ratio on the adsorption of CIP by the intercalated composite C1M1.5C

Figure 6 shows that the adsorption of CIP by ZBC composite with MT was significantly higher than

that when used alone. The adsorption and removal of composite R1.5M1D reached 192.11 mg/g and 69%, respectively, which was 1.5 times higher than that of ZBC. Therefore, the optimum composite ratio for the pyrolysis method was montmorillonite:biochar 1.5:1. Figure 7 shows that the adsorption of CIP by the intercalated composite C2M1C was also higher than that of ZBC and MT, and its maximum adsorption amount was 218.44 mg/g, which was two times that of ZBC, suggesting that the optimum composite ratio for the intercalation method was montmorillonite:biochar 2:1. The ratio of the composites prepared by the pyrolysis method to those prepared by the intercalation method was higher than that of surface area, and adsorption sites increased, which significantly enhanced the removal of CIP.

### 3.2.2 Effect of dosage on adsorption effect

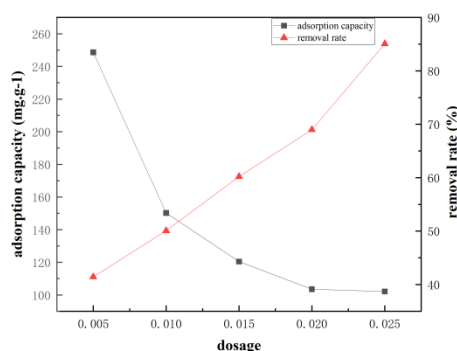


Figure 8 The effect of R1.5M1D dosage on the adsorption of CIP

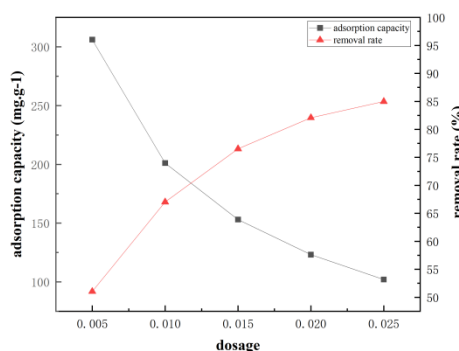


Figure 9 The effect of C2M1C dosage on the adsorption of CIP

Figure 8 shows that with the increase of pyrolysis composite R1.5M1D dosage, its adsorption of CIP decreased, but the removal rate increased, indicating that the removal effect is related to the dosage. The surface of the composite material was gradually occupied by CIP molecules, reaching adsorption saturation, and the adsorption amount tended to stabilize. When increasing the dosage, the adsorption sites increased, but the total adsorption amount remained unchanged, resulting in a decrease in the adsorption amount per unit mass. At the dosage of 0.025 g, the removal rate reached 89%, which was the maximum value. Therefore, 0.025 g was the optimal dosage at a CIP concentration of 30 mg/L and a solution volume of 100 mL.

Figure 9 shows that the adsorption amount and removal rate of the intercalated composite C2M1C showed similar trends with the dosage. The rate of decrease in adsorption is high in the interval of 0.005-0.01 g of dosage, while the decrease and increase in adsorption and removal rate are low in the interval of 0.02-0.025 g. The decrease and increase in adsorption and removal rate are low in the interval of 0.005-0.01 g of dosage. Too little dosage results in a low removal rate, and too much results in adsorbent surplus. The adsorption amount and removal rate reached 123.13 mg/g and 85%, respectively, at a dosage of 0.02 g. Therefore, 0.02 g is a more appropriate dosage under the premise of ensuring the removal effect.

### 3.2.3 Effect of pH on adsorption

Figure 10 shows that the adsorption amount and removal rate of CIP by the composite R1.5M1D increased and then decreased with the increase of pH, leveled off and then increased. The adsorption amount and removal rate increased in the pH 2~4 and 8~10 intervals, and reached the highest at pH 10 with 107.81 mg/g and 90%, respectively, which were 20% and 18% higher than that at pH 2, respectively. Figure 11 shows that the adsorption and removal of CIP by the composite C2M1C increased and then stabilized with the increase of pH, and the fluctuation was larger in the interval of pH 2~8. The adsorption and removal of CIP by the composite C2M1C were the highest at pH 10, with the values of 139.45 mg·g<sup>-1</sup> and 92.29%, which indicated that the alkaline environment (pH=10) was conducive to the adsorption of CIP by the composite C2M1C.

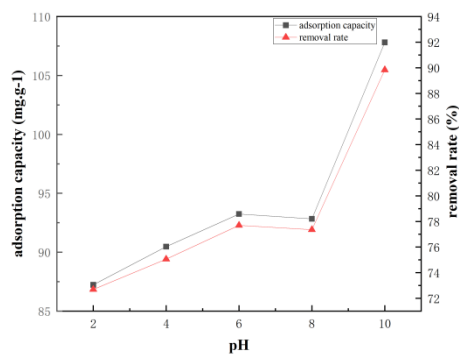


Figure 10 The effect of pH on CIP adsorption by R1.5M1D

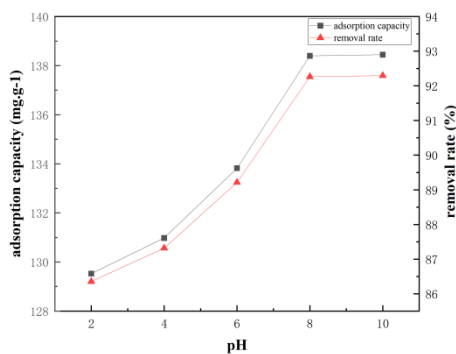


Figure 11 The effect of pH on CIP adsorption by C2M1C

3.2.4 Effect of initial adsorption concentration on adsorption effect

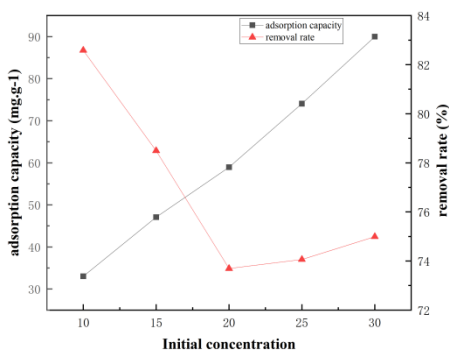


Figure 12 The effect of initial concentration on CIP adsorption by R1.5M1D

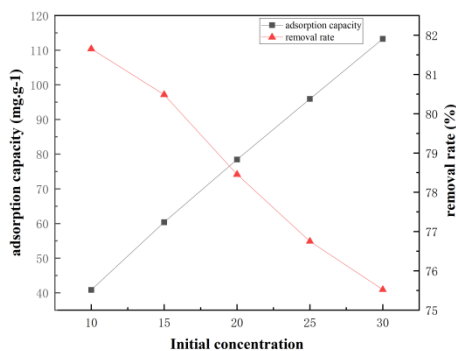


Figure 13 The effect of initial concentration on CIP adsorption by C2M1C

Figures 12 and 13 show that the adsorption of CIP by the intercalation and pyrolysis composites increased and the removal rate decreased with increasing solution concentration. The pyrolysis composite R1.5M1D showed a steady increase in adsorption of about 2% over the concentration range of 10 to 30 mg/L, with slight fluctuations in the removal rate, but the overall trend was not affected. At a concentration of 30 mg/L, the adsorption amount reached 90 mg/g, and the removal rate was 75%, indicating sufficient adsorption sites for the composite. Therefore, 30 mg/L was the optimal initial concentration for the CIP solution. In Fig. 4.13, the adsorption amount increased with the increase of initial concentration and reached 113.94 mg/L at 30 mg/L, and the removal rate gradually decreased and leveled off. The adsorption amount grows fast with more adsorption sites at low concentrations, but with the increase of adsorbent, the adsorption sites decrease and the removal rate tends to stabilize. Therefore, 30 mg/L is a suitable choice for the initial concentration.

3.2.5 Effect of adsorption time on adsorption effect

Figures 14 and 15 show that the adsorption and removal rates of pyrolysis and intercalation composites increased and then slowed down with the extension of time. The removal rate and adsorption amount increased faster from 0 to 180 min, and the removal rate could reach up to 73% and the adsorption amount reached 86.90 mg/g and 109.64 mg/g, respectively, at 180 min. From 180 to 300 min, the removal rate and the adsorption amount continued to increase, but the growth rate slowed down. This indicates that the composites provided a large number of binding sites for CIP in the initial stage, while the adsorption process stabilized after 180 min when the adsorption sites were gradually saturated and the mass transfer rate decreased [7]. Therefore, the

optimum adsorption time for both composites is 180 min.

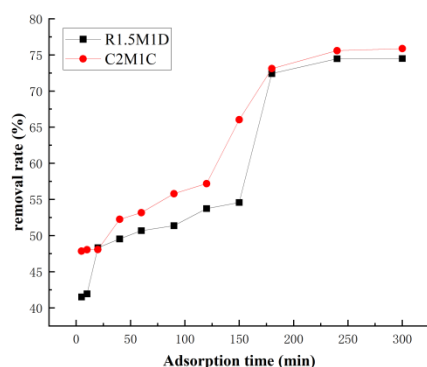


Figure 14 The effect of adsorption time on removal rate

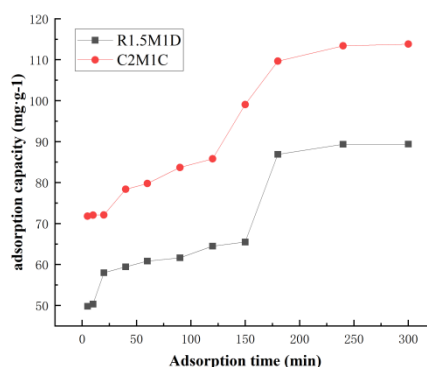


Figure 15 The effect of adsorption time on the adsorption capacity

### 3.2.6 Effect of adsorption temperature on adsorption effect

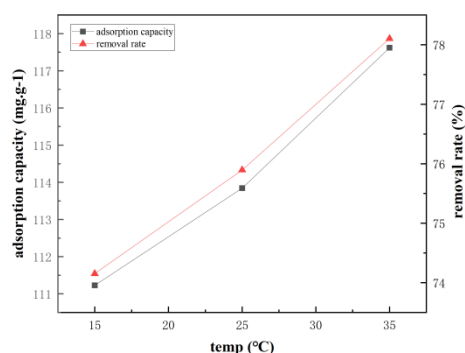


Figure 16 The effect of ambient temperature on CIP adsorption by R1.5M1D

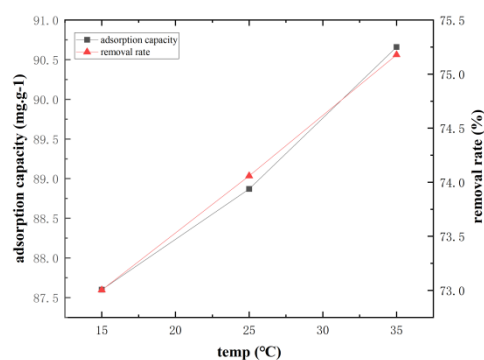


Figure 17 The effect of ambient temperature on CIP adsorption by C2M1C

The adsorption performance of the composites on CIP was investigated at 15 °C, 25 °C, and 35 °C, and the results are shown in Figures 16 and 17. The results showed that the removal rate and adsorption amount of CIP by the composites increased with the increase of the temperature, and the increase was especially large in the interval of 15–25 °C. At 35 °C, the adsorption amounts reached 90.66 mg/g and 117.62 mg/g, which were significantly increased compared with those at 15 °C. At 35 °C, which was significantly higher than that at 15 °C. The increase in temperature led to the intensification of CIP molecular movement, which increased the chance of collision with the adsorbent material and at the same time promoted the molecules to cross the boundary layer and internal diffusion. The elevated temperature favors the molecular movement and enhances the adsorption capacity of the adsorbent. The adsorption process of composites is heat-absorbing and can be analyzed in conjunction with adsorption thermodynamics [8].

### 3.2.7 Adsorption kinetics

(1) *Kinetic studies of quasi-primary and quasi-secondary adsorption.* The data related to the fitting of the quasi-primary and quasi-secondary equations for the pyrolysis composite R1.5M1D and the intercalation composite C2M1C adsorbed CIP are shown in Table 4.

makings	$Q_{\text{exp}}$ ( $\text{mg}\cdot\text{g}^{-1}$ )	quasi-level equation (math.)			quasi-secondary equation (math.)		
		$q_e$ ( $\text{mg}\cdot\text{g}^{-1}$ )	$k_f$ ( $\text{min}^{-1}$ )	$R_{\text{adj}}^2$	$q_e$ ( $\text{mg}\cdot\text{g}^{-1}$ )	$k_s$ ( $\text{g}\cdot(\text{mg}\cdot\text{min})^{-1}$ )	$R_{\text{adj}}^2$
R1.5M1D	89.39	93.80	$2.24\times 10^{-2}$	0.66990	32.39	$5.72\times 10^{-3}$	0.99832
C2M1C	113.80	77.02	$1.66\times 10^{-2}$	0.79325	117.79	$4.35\times 10^{-4}$	0.99165

Table 4 Adsorption kinetic parameters of R1.5M1D、C2M1C for CIP

Table 4 shows that the quasi-secondary kinetic correlation coefficients,  $R_2$ , of the pyrolysis and intercalation composites are 0.99832 and 0.99165, respectively, which are much higher than those of the quasi-primary model. The measured adsorption amounts of these two composites were 32.39 and 117.79 mg/g, respectively, and the equilibrium adsorption amounts were 89.39 and 113.80 mg/g, respectively, which were similar values, indicating that the quasi-secondary kinetic model was more suitable for describing the adsorption process of their CIP.

(2) *Intra-particle diffusion model*. The slower adsorption process is the main factor affecting the rate of adsorption.

methodologies	Phase I		Phase II	
	$k_i$ ( $\text{mg}\cdot\text{g}^{-1}\cdot\text{min}^{-0.5}$ )	$R_{\text{adj}}^2$	$k_i$ ( $\text{mg}\cdot\text{g}^{-1}\cdot\text{min}^{-0.5}$ )	$R_{\text{adj}}^2$
R1.5M1D	1.52116	0.89640	0.65319	0.79160
C2M1C	1.75662	0.96156	2.61839	0.73213

Table 5 Intra-particle diffusion parameters of R1.5M1D、C2M1C for CIP

Table 5 shows that the two composites adsorbed CIP in two phases. The first phase adsorption rate constant of pyrolytic composite R1.5M1D, 1.52116, is greater than the second phase, 0.65319. On the contrary, the first phase adsorption rate constant of the intercalated composite C2M1C, 1.75662, is less than that of the second phase, 2.61839. This suggests that the second phase of the adsorption of R1.5M1D and the first phase of the adsorption of C2M1C are critical for the adsorption of CIP by the respective materials. CIP is critical. Moreover, the rate of intra-particle diffusion is not the only controlling step.

### 3.2.8 Adsorption isotherm studies

temp( $^{\circ}\text{C}$ )	$Q_{\text{me}}$ ( $\text{mg}\cdot\text{g}^{-1}$ )	Langmuir			Freundlich		
		$Q_{\text{max}}$ ( $\text{mg}\cdot\text{g}^{-1}$ )	$K_L$ ( $\text{L}\cdot\text{mg}^{-1}$ )	$R_{\text{adj}}^2$	$\frac{1}{n}$	$K_f$ ( $\text{mg}\cdot\text{g}^{-1}\cdot(\text{mg}\cdot\text{L}^{-1})^{-1/n}$ )	$R_{\text{adj}}^2$
15	37.12	43.99	0.73	0.91	-0.24	22.99	0.78
25	39.14	45.58	0.74	0.97	-0.25	23.34	0.89
35	40.82	45.63	0.95	0.97	-0.23	25.22	0.95

marginal notes: “ $Q_{\text{me}}$ ” is an experimental measurement,  $\text{mg}\cdot\text{g}^{-1}$ .

Table 6 R1.5M1D composites adsorption isotherm parameters for CIP

temp( $^{\circ}\text{C}$ )	$Q_{\text{me}}$ ( $\text{mg}\cdot\text{g}^{-1}$ )	Langmuir			Freundlich		
		$Q_{\text{max}}$ ( $\text{mg}\cdot\text{g}^{-1}$ )	$K_L$ ( $\text{L}\cdot\text{mg}^{-1}$ )	$R_{\text{adj}}^2$	$\frac{1}{n}$	$K_f$ ( $\text{mg}\cdot\text{g}^{-1}\cdot(\text{mg}\cdot\text{L}^{-1})^{-1/n}$ )	$R_{\text{adj}}^2$
15	56.86	63.46	1.096	0.96	0.18	39.15	0.84
25	57.75	64.91	1.066	0.97	0.19	39.35	0.85
35	57.87	64.28	1.274	0.94	0.17	41.34	0.80

marginal notes: “ $Q_{\text{me}}$ ” is an experimental measurement,  $\text{mg}\cdot\text{g}^{-1}$ .

Table 7 C2M1C adsorption isotherm parameters for CIP

Table 6 shows that the correlation coefficients of both the Freundlich and Langmuir adsorption models

for the pyrolyzed composite R1.5M1D increased as the temperature increased, and the correlation coefficients of the Langmuir model were consistently higher than those of the Freundlich model. At 25 °C, the correlation coefficient of the Freundlich model was 0.891, which was much lower than that of the Langmuir model of 0.967. This indicated that the adsorption of CIP by R1.5M1D was more consistent with the Langmuir model.

According to Table 7, the correlation coefficients of the Langmuir model are all larger than the Freundlich model, and the correlation coefficients of the Freundlich model are all numerically smaller than 0.9. Based on the small difference between the curve-fitting value of  $Q_{max}$  and the measured value of  $Q_{me}$ , it can be concluded that the adsorption of CIP by interpolated composites is more consistent with the Langmuir model. In addition, the adsorption coefficient  $K_f$  increases with increasing temperature, indicating that warming is favorable to the adsorption of CIP by the composites. From the table, it can also be concluded that the  $1/n$  values are all less than 0.5, indicating that the adsorption reaction is easier.

### 3.2.9 Adsorption thermodynamics

In order to study the adsorption process and mechanism, Gibbs free energy change  $\Delta G$ , enthalpy change  $\Delta H$ , and entropy change  $\Delta S$  were calculated at different temperatures (288 K, 298 K, and 308 K) to analyze the thermodynamic properties of adsorption. The relevant parameters are shown in Table 8.

makings	temp (K)	$\Delta G$ (kJ·mol <sup>-1</sup> )	$\Delta H$ (kJ·mol <sup>-1</sup> )	$\Delta S$ (kJ·mol <sup>-1</sup> ·K <sup>-1</sup> )
R1.5M1D	288	-7.51	3.441	0.038
	298	-7.80		
	308	-8.27		
C2M1C	288	-8.78	2.026	0.038
	298	-9.10		
	308	-9.53		

Table 8 Adsorption thermodynamic parameters of R1.5M1D、C2M1C for CIP

According to Table 8, the free energy changes  $\Delta G$  of both composites at three different ambient temperatures were negative, indicating that the adsorption of CIP by these composites was spontaneous. In addition, the  $\Delta G$  values decreased with increasing temperature, indicating that the adsorption process was promoted by increasing temperature.

The  $\Delta G$  values were all located in the interval from -20 to 0 kJ/mol, indicating that the adsorption processes were all physisorption in nature.

The  $\Delta H$  values were all positive, indicating that this adsorption process is a heat-absorbing reaction, and hence an increase in temperature helps in promoting the adsorption.

The  $\Delta S$  values are all greater than zero, implying that the adsorption process is accompanied by an increase in entropy and an increase in the disorder of the system, thus making the adsorption process more stable [10].

### 3.2.10 Composite material recycling performance

The saturated composite was desorbed into 0.01 mol/L HCl for 4 h. The process was repeated five times after washing and drying, and the adsorption was calculated.

Figure 18 shows that the adsorption capacity of the composites continued to decrease during recycling. The adsorption of both composites, R1.5M1D and C2M1C, decreased from 89.457 and 114.782 mg/g at the first time to 16.237 and 24.353 mg/g at the fifth time, with a decrease of about 81% and 78%, respectively. This decrease may be attributed to the difficulty of desorption of CIP molecules and the damage of the pore structure due to the repeated action of HCl solution.

### 3.2.11 Adsorption mechanism

The adsorption mechanism was analyzed by combining the characterization methods as well as adsorption mechanics, adsorption isotherms, and intra-particle diffusion models. The adsorption

mechanism of CIP by pyrolytic composite R1.5M1D and intercalated composite C2M1C is hypothesized as follows:

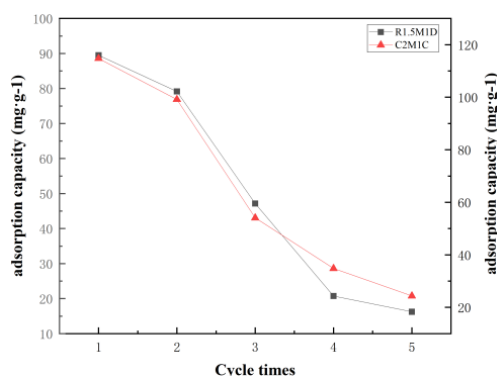


Figure18 Recycle ability of composites to adsorb CIP

When the composite material is added into the CIP solution, the aromatic ring on the CIP sub-surface combines with the composite material surface -OH, C=C and other functional groups to form the hydrogen bond; according to the previous study on the adsorption effect of pH, it is found that the pH affects the adsorption amount and removal rate of the composite material, so it can be deduced that electrostatic attraction is also the main influencing factor of the adsorption process; the composite material has a larger specific surface area compared to a single material and a richer pore structure, meanwhile, the composite material has a larger specific surface area and a richer pore structure than a single material. The composite material has a larger specific surface area and a richer pore structure than the single material, and the adsorption process is more composite with the quasi-secondary kinetic model. The increase of adsorption sites is favorable for the adsorption process, and the adsorption equilibrium state will be reached when the adsorption sites are almost completely occupied [11].

#### 4. Deliberations

The main study of the thesis analyzed the adsorption of ciprofloxacin hydrochloride (CIP) by biochar/montmorillonite composites, which is still deficient due to time limitation:

- No small trials were carried out on other adsorbents such as methyl violet, tetracycline hydrochloride, Pb, etc.
- The prepared pyrolytic composites were not further investigated on the ratio of biochar to montmorillonite.
- The number of replicates in the study of cycling properties of biochar/composites is too low, and low consumable activation methods need to be found.

#### 5. Reach a Verdict

Biochar/montmorillonite composites with different ratios were prepared from zinc chloride-modified rice husk biochar and sodium-based montmorillonite by both intercalation and pyrolysis and characterized by X-ray diffraction, Fourier transform infrared (FTIR) spectroscopy, BET test, and scanning electron microscopy. The adsorption properties of the composites on ciprofloxacin hydrochloride (CIP) were also investigated by adsorption experiments, and the following conclusions were drawn:

- The composites showed better removal and adsorption of CIP than single material.
- The optimal composite ratios of montmorillonite and biochar for pyrolysis and intercalation were 1.5:1 and 2:1, respectively, and the adsorption capacity and removal rate of composite R1.5M1D reached 192.11 mg/g and 69%, which were 1.5 times of the lowest adsorption ZBC, and the adsorption capacity of composite C2M1C reached 218.44 mg/g, which was two times of the lowest adsorption ZBC.

- c) The two composites showed better adsorption performance of CIP at a solution concentration of 30 mg/L and in an alkaline environment (pH = 10).
- d) The specific surface area of pyrolytic composite R1.5M1D and intercalated composite C2M1C reached 86.2830 m<sup>2</sup>.g<sup>-1</sup> and 246.7287 m<sup>2</sup>.g<sup>-1</sup>, respectively, which were 94% and 98% higher compared to ZBC with the lowest value, and the composites were present with the presence of -OH, C=O, and C=C functional groups.
- e) Both composites conform to the quasi-secondary kinetic model, and the adsorption process is a number of controlled steps such as heat absorption, entropy increase, and particle-containing diffusion. The adsorption of CIP by composites C2M1C and R1.5M1D is more consistent with the Langmuir isothermal adsorption model.
- f) The cyclic adsorption performance of composites C2M1C and R1.5M1D both decreased with the number of cycles, and all of them showed a large decrease in the third time.

## 6. Reference

- [1] Yang Wenhuan, Wang Chaohui, Gao Naiyun, et al. Research Progress on Advanced Oxidation Removal Methods of Ciprofloxacin in Water [J]. Applied Chemical Industry, 2016, 45(10):1959-1964+1968. DOI:10.16581/j.cnki.issn1671-3206.20160705.007. (in chinese)
- [2] Liu Qi. Study on the degradation of ciprofloxacin wastewater by iron oxide-activated persulfate [D]. Nanjing Forestry University, 2023. DOI:10.27242/d.cnki.gnjlu.2023.000523. (in chinese)
- [3] Pang Shuqiang. Structural Design of Biochar Materials and Their Catalytic Degradation of Ciprofloxacin by Persulfate Oxidation [D]. Qingdao University, 2023. DOI:10.27262/d.cnki.gqdau.2023.001848. (in chinese)
- [4] Yu Shanshan. ZnO/Vo-(111)Cu<sub>2</sub>O/NiF<sub>2</sub> Synergistic Photocatalytic Material with PMS Oxidation for Efficient Removal of Ciprofloxacin Hydrochloride [J]. Shandong Chemical Industry, 2024, 53(10):34-36. DOI:10.19319/j.cnki.issn.1008-021x.2024.10.009. (in chinese)
- [5] Guo Yakai. Study on the Preparation of Sludge-based Biochar and Its Adsorption of Ciprofloxacin Hydrochloride [D]. Chang'an University, 2021. DOI:10.26976/d.cnki.gchau.2021.001795. (in chinese)
- [6] Liu Q S, Zheng T, Li N, et al. Modification of bamboo-based activated carbon using microwave radiation and its effects on the adsorption of methylene blue [J]. Applied Surface Science: A Journal Devoted to the Properties of Interfaces in Relation to the Synthesis and Behaviour of Materials, 2010, 256(10):3309-3315.
- [7] Xiong Qingyue. Study on the Preparation and Modification of Peanut Shell Biochar and Its Adsorption Performance for Typical Antibiotics in Water [D]. Gansu: Lanzhou University of Technology, 2023. (in chinese)
- [8] Chen Chaofan. Study on the Efficiency and Mechanism of Phosphorus Adsorption by Calcium and Magnesium Modified Rice Husk-Sludge Biochar [D]. Heilongjiang: Harbin Institute of Technology, 2022. (in chinese)
- [9] Akhtar M, Bhanger M I, Iqbal S, et al. Sorption potential of rice husk for the removal of 2,4-dichlorophenol from aqueous solutions: kinetic and thermodynamic investigations [J]. Journal of Hazardous Materials, 2006, 128(1):44-52.
- [10] Yang Lin, Wu Pingxiao, Liu Shuai, et al. Study on the adsorption performance of gender-modified montmorillonite for cadmium and tetracycline in water [J]. Acta Scientiarum Circumstantiae, 2016, 36(6):2033-2042. (in chinese)
- [11] Research on the Adsorption Characteristics and Mechanism of Lead and Cadmium Pollution by Li Beibei. Biochar/Attapulgite Composite Materials [D]. Southeast University, 2022. DOI:10.27014/d.cnki.gdnau.2022.001942. (in chinese)
- [12] Wu Peng. Preparation of Carbon Quantum Dots from Cellulose via Hydrothermal Carbonization and Study on Their Fluorescence Mechanism and Properties [D]. Northeast Forestry University, 2019. DOI:10.27009/d.cnki.gdblu.2019.000027. (in chinese)